Springer

KSME

Journal of Mechanical Science and Technology 31 (11) (2017) 5081~5087
www.springerlink.com/content/1738-494x(Print)/1976-3824(Online)
DOI 10.1007/s12206-017-1001-8

Heat transfer and gas-solid behaviors in pneumatic transport reactor used of carbon capture system †

Seungyeong Choi[1], Hoanju Yoo[2], Hokyu Moon[3], Yong-Ki Park[4] and Hyung Hee Cho[1,*]

[1]*Department of Mechanical Engineering, Yonsei University, 50 Yonsei-ro, Seodaemun-gu, Seoul 03722, Korea*
[2]*Aircraft Research & Development Division, Korea Aerospace Industries Ltd., 78, Gongdan 1-ro, Sanam-Myun, Sacheon, Gyeongnam 52529, Korea*
[3]*Tokamak Engineering Department, National Fusion Research Institute (NFRI), 169-168 Gwahak-ro, Yuseong-gu, Daejeon 34133, Korea*
[4]*Green Chemistry Process Research Division, Korea Research Institute of Chemical Technology, Ganjeongro 141, Daejeon 34114, Korea*

(Manuscript Received April 5, 2017; Revised August 4, 2017; Accepted August 21, 2017)

Abstract

A pneumatic transport reactor can be used for continuous carbon capture processes using a dry sorbent because it can handle large quantities of flue gas. To design efficient reactors, it is necessary to understand the internal characteristics of a reactor with a complicated gas-solid flow. Computational fluid dynamics using an Eulerian-Eulerian approach was adopted to simulate gas-solid two-phase flow to better understand the gas-solid behaviors and heat transfer characteristics in a pneumatic transport reactor. Numerical simulations were used to analyze the pressure difference, solid mass flux, and heat transfer coefficient. The results showed that the gas-solid behavior was unstable and that localized particle flow affects the heat transfer characteristics. The degree of particle mixing near the solid return inlet was lower than that at greater heights within the reactor; in the inlet region, the heat transfer coefficient is not uniform in accordance with the non-uniformity of solid particle behavior.

Keywords: CO_2 capture; Pneumatic transport; Gas-solid behaviors; Heat transfer

1. Introduction

Carbon dioxide is believed to be the main cause of global warming. Since industrialization, the atmospheric CO_2 concentration has risen with anthropogenic emissions of CO_2. Most CO_2 emissions are currently from coal-fired power plants [1, 2]. However, the number of coal-fired power plants will not be reduced soon due to the current industrial structure and the low efficiency of alternative energy. Consequently, there has been much effort to reduce CO_2 emissions from power plants using carbon capture and sequestration technology [3, 4]. Carbon capture technology consisting of two gas-solid fluidized beds using a dry sorbent has many advantages: It can accommodate the massive throughput of flue gas from a power plant using a continuous process; it does not use steam; and the reactor is compact [5, 6]. From a thermal perspective, thermal equilibrium in each reactor must be maintained for continuous operation [7]. The process itself involves two reactions: cooling carbonation for CO_2 capture and regeneration using the desorption energy of captured CO_2, as shown in Fig. 1. Reducing the desorption energy is essential for cost-effective processing and must be addressed for commercialization. To save energy in CO_2 capture reactions, there are two heat exchangers on the outer wall of the reactor: The reaction

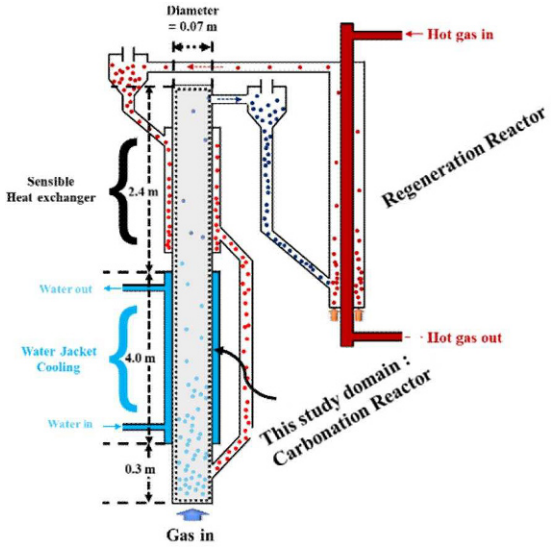

Fig. 1. Schematic geometry of the continuous process in a carbon-capture system using dry sorbent.

*Corresponding author. Tel.: +82 2 2123 2828
E-mail address: hhcho@yonsei.ac.kr
This paper was presented at the ISFMFE 2016, LOTTE City Hotel, Jeju, Korea, October 18-22, 2016. Recommended by Guest Editor Hyung Hee Cho.

heat exchanger and sensible heat exchanger.

Many methods have been suggested, including a calcium looping process [7] and multi-stage heat-exchangeable reactor systems [6, 8, 9], to achieve continuous carbon capture. The operating conditions of these systems must be optimal for effective processing; however, depending on the given properties of the gas and sorbent, the conditions differ and must be analyzed [10].

A pneumatic transport reactor can run continuously because the sorbent particles can leave the reactor with sufficient momentum. For the pneumatic transport reactor to operate properly, the reactor should be designed as considering required reacting condition. Good gas-solid mixing and sufficient particle residence time are required. Especially, because the carbonation and regeneration process are the exothermic and endothermic reaction, respectively, controlling the reactor temperature condition is the most critical when applying the temperature swing absorption process [10]. To control the temperature condition in the reactor, heat exchange between the gas-solid flow and the reactor should be estimated. From this design perspective, it is necessary to analyze the complex gas-solid behaviors and heat transfer processes in the reactor [11-13]. Therefore, this study examined the effectiveness of a pneumatic transport reactor using numerical simulations to analyze the pressure difference in the reactor, sorbent behaviors, and the bed-to-wall heat transfer coefficient. The characteristics of two-phase flow and single-phase gas flow were compared.

2. Pneumatic transport reactor

Continuous gas-solid reaction processes can be divided into moving bed, fluidized bed, and pneumatic transport systems. Unlike the last two, in a moving bed, solid particles are conveyed mechanically or under the force of gravity, with the aid of a rotation machine, agitator, or vibrator. In a fluidized bed, the solid particles are blown by gas flow, and back-mixing occurs in the bed. Suspended particles in the reactor exhibit stochastic behavior, leaving the reactor randomly regardless of the order of injection. In pneumatic transport, the gas flow carries dilute solid particles in one direction, like a piston. When particles of uniform size are introduced simultaneously, the particles have the same residence times in the reactor. The latter two systems are largely overlapping, as shown in Fig. 2 [11]. It is easy to distinguish the two systems theoretically, while it is difficult in industrial practice.

Generally, solid particles start to move apart when they exceed the terminal velocity, as described by Stokes law at low Reynolds numbers:

$$U_t = g\rho_s d_p^2 / 18\mu . \quad (1)$$

Particles can scatter in the reactor. The boundary conditions that distinguish a fluidized bed and pneumatic transport are the minimum transport velocity and minimum pressure-drop

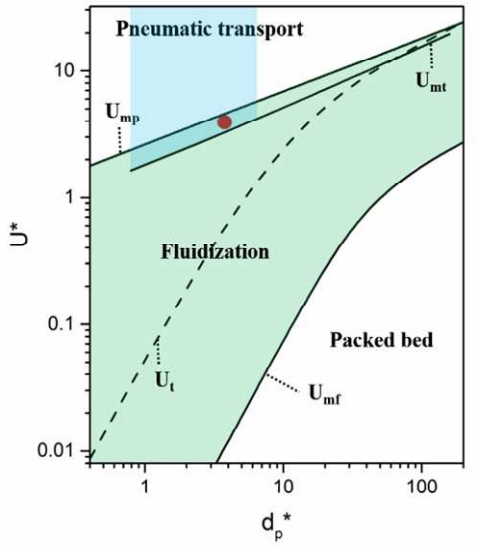

Fig. 2. Idealized flow regime map for gas-solids upward transport [13].

velocity, expressed as follows [14]:

$$U_{mt} = \frac{\mu Re_{se}}{d_p \rho_g} + \frac{G_s \varepsilon_{CA}}{\rho_p (1-\varepsilon_{CA})} \quad (2)$$

$$Re_{se} = 1.53 Ar^{0.5} \quad (3)$$

$$U_{mt} = 10.1 (g d_p)^{0.347} \left(\frac{G_s}{\rho_g}\right)^{0.310} \left(\frac{d_p}{D}\right)^{-0.139} Ar^{-0.021} . \quad (4)$$

Pneumatic transport reactor involves dilute gas-solid mixtures and is suitable for rapid reactions which is incorporated into the upward flow of solids circulations systems. When analyzing a pneumatic transport reactor, the important factors are the pressure difference loss, gas-solid behaviors, and energy balance, which influence the long-term operating costs of the entire system [11, 13].

3. Research method

3.1 Numerical simulation

To analyze the multiphase flow in a pneumatic transport reactor involving gas-solid, a Computational fluid dynamics (CFD) simulation was used. Using ANSYS Fluent 16.0 software, the Eulerian-Eulerian method was used for an unsteady simulation with a fixed time step of 10^{-3} second. To quantify complex multiphase flow that changes instantaneously, time-averaged values were analyzed after the flow reached a quasi-steady state. In the Eulerian-Eulerian method, the gas and solid are assumed to be interpenetrating continua, and the conservation of mass, momentum, and energy for each phase is solved. To analyze the motion of granular particles within the reactor, the Kinetic theory of granular flow (KTGF) was applied.

To conserve momentum, various external forces should be

Table 1. Summary of the governing and constitutive equations.

Conservation of mass

Gas phase: $\frac{\partial}{\partial t}\left(\varepsilon_g \rho_g\right)+\nabla\cdot\left(\varepsilon_g \rho_g \vec{v}_g\right)=0$

Solid phase: $\frac{\partial}{\partial t}\left(\varepsilon_s \rho_s\right)+\nabla\cdot\left(\varepsilon_s \rho_s \vec{v}_s\right)=0$

Conservation of momentum

Gas phase: $\frac{\partial}{\partial t}\left(\varepsilon_g \rho_g \vec{v}_g\right)+\nabla\cdot\left(\varepsilon_g \rho_g \vec{v}_g \vec{v}_g\right)=-\varepsilon_g \nabla p+\nabla\cdot\bar{\bar{\tau}}_g+\varepsilon_g \rho_g \vec{g}+K_{gs}\left(\vec{v}_g-\vec{v}_s\right)$

Solid phase: $\frac{\partial}{\partial t}\left(\varepsilon_s \rho_s \vec{v}_s\right)+\nabla\cdot\left(\varepsilon_s \rho_s \vec{v}_s \vec{v}_s\right)=-\varepsilon_s \nabla p-\nabla p_s+\nabla\cdot\bar{\bar{\tau}}_s+\varepsilon_s \rho_s \vec{g}-K_{gs}\left(\vec{v}_g-\vec{v}_s\right)$

Conservation of energy

Gas phase: $\frac{\partial}{\partial t}\left(\varepsilon_g \rho_g h_g\right)+\nabla\cdot\left(\varepsilon_g \rho_g \vec{v}_g h_g\right)=\varepsilon_g \frac{\partial p_g}{\partial t}+\bar{\bar{\tau}}_g:\nabla\vec{u}_g-\nabla\cdot\vec{q}_g+Q_{sg}$

Solid phase: $\frac{\partial}{\partial t}\left(\varepsilon_s \rho_s h_s\right)+\nabla\cdot\left(\varepsilon_s \rho_s \vec{v}_s h_s\right)=\varepsilon_s \frac{\partial p_s}{\partial t}+\bar{\bar{\tau}}_s:\nabla\vec{u}_s-\nabla\cdot\vec{q}_s+Q_{gs}$

Constitutive equations (Kinetic theory to granular flows (KTGF))

Conservation of granular temperature (Algebraic formulation):

$$\Theta_s=\frac{1}{3}u_{s,i}u_{s,i}$$

$$\frac{3}{2}\left[\frac{\partial}{\partial t}\left(\varepsilon_s \rho_s \Theta_s\right)\right]=\left(-p_s \bar{\bar{I}}+\bar{\bar{\tau}}_s\right):\nabla\vec{v}_s+\nabla\cdot\left(k_{\Theta_s}\nabla\Theta_s\right)-\gamma_{\Theta_s}+\phi_{gs}$$

$$k_{\Theta_s}=\frac{150\rho d_s\sqrt{(\Theta\pi)}}{384\left(1+e_{ss}\right)g_{0,ss}}\left[1+\frac{6}{5}\varepsilon_s g_{0,ss}\left(1+e_{ss}\right)\right]^2+2\rho_s\varepsilon_s^2 d_s\left(1+e_{ss}\right)g_{0,ss}\sqrt{\frac{\Theta_s}{\pi}}\quad\text{(Gidaspow et al.)}$$

$$\phi_{gs}=-3K_{gs}\Theta_s$$

$$\gamma_{\Theta_s}=\frac{12\left(1-e_{ss}^2\right)g_{0,ss}}{d_s\sqrt{\pi}}\rho_s\varepsilon_s^2\Theta_s^{3/2}\quad\text{(Lun et al.)}$$

Phase stress-strain tensor

Gas phase: $\bar{\bar{\tau}}_g=\varepsilon_g\mu_g\left(\nabla\vec{v}_g+\nabla\vec{v}_g^{\,T}\right)-\frac{2}{3}\varepsilon_g\mu_g\nabla\cdot\vec{v}_g\bar{\bar{I}}$

Solid phase: $\bar{\bar{\tau}}_s=\varepsilon_s\mu_s\left(\nabla\vec{v}_s+\nabla\vec{v}_s^{\,T}\right)+\varepsilon_s\left(\lambda_s-\frac{2}{3}\mu_s\right)\nabla\cdot\vec{v}_g\bar{I}$

μ_g : Gas phase viscosity

$$\mu_s=\frac{4}{5}\varepsilon_s\rho_s d_s g_{0,ss}\left(1+e_{ss}\right)\left(\frac{\Theta_s}{\pi}\right)^{\frac{1}{2}}+\frac{10\rho_s d_s\sqrt{\Theta_s\pi}}{96\varepsilon_s\left(1+e_{ss}\right)g_{0,ss}}\left[1+\frac{4}{5}g_{0,ss}\varepsilon_s\left(1+e_{ss}\right)\right]^2\quad\text{(Gidaspow et al.)}$$

$$\lambda_s=\frac{4}{3}\varepsilon_s d_s g_{0,ss}\left(1+e_{ss}\right)\left(\frac{\Theta_s}{\pi}\right)^{1/2}\quad\text{(Lun et al.)}$$

Solid pressure (Lun et al.): $p_s=\varepsilon_s\rho_s\Theta_s+2\rho_s\left(1+e_{ss}\right)\varepsilon_s^2 g_{0,ss}\Theta_s$

Radial Distribution (Lun et al.): $g_0=\left[1-\left(\frac{\varepsilon_s}{\varepsilon_{s,max}}\right)^{\frac{1}{3}}\right]^{-1}$

Shear force at the wall for granular phase: $\vec{\tau}_s=-\frac{\pi}{6}\sqrt{3}\phi\frac{\varepsilon_s}{\varepsilon_{s,max}}\rho_s g_0\sqrt{\Theta_s}\overrightarrow{U_{s\|}}$

General boundary condition for granular temperature at wall: $q_s=\frac{\pi}{6}\sqrt{3}\phi\frac{\varepsilon_s}{\varepsilon_{s,max}}\rho_s g_0\sqrt{\Theta_s}\overrightarrow{U_{s\|}}\cdot\overrightarrow{U_{s\|}}-\frac{\pi}{4}\sqrt{3}\frac{\varepsilon_s}{\varepsilon_{s,max}}\left(1-e_{sw}^2\right)\rho_s g_0\Theta_s^{3/2}$

Interphase momentum exchange coefficient (Gibilaro model): $K_{gs}=\left(\frac{18}{Re_s}+0.33\right)\frac{\rho_g\left|v_s-v_g\right|}{d_p}\varepsilon_s\varepsilon_g^{-1.8}$

Interphase heat exchange coefficient (Gunn model)

$$Nu_s=\left(7-10\varepsilon_g+\varepsilon_g^2\right)\left(1+0.7Re_s^{0.2}Pr^{\frac{1}{3}}\right)+\left(1.33-2.4\varepsilon_g+1.2\varepsilon_g^2\right)Re_s^{0.7}Pr^{1/3}\ \ (Re_s<10^5)$$

$$Re_s=\frac{\rho_g d_s\varepsilon_g\left|v_g-v_s\right|}{\mu_g},\ Pr=\frac{\mu_g C_{s,g}}{k_g}$$

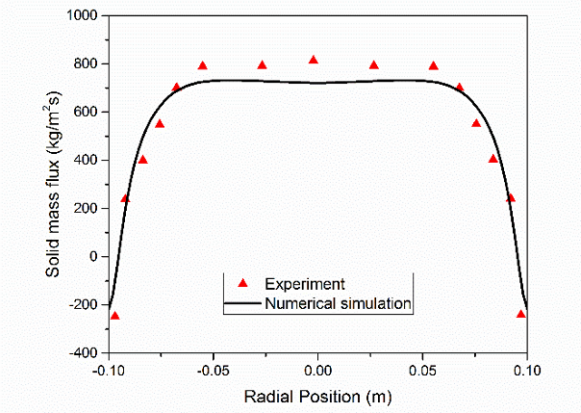

Fig. 3. Validation comparing numerical simulation data and experimental data [16].

considered. The virtual mass force and lift force are negligible because the density of the primary phase of the gas is smaller than that of the secondary phase of the solid, and the particle size is sufficiently small. The interaction force between phases must be described accurately. The Gibilaro drag force model was used, which is generalized for fluid-particle interactions [15].

The energy conservation equation must consider the heat exchange between the gas and solid. The Gunn heat exchange model was used for granular flows [16]. A cold flow simulation does not consider chemical reactions. The fluctuating energy of a particle is expressed using the granular temperature, which is proportional to the kinetic energy of the particles' random motion. Detailed equations are described in Table 1.

3.2 Model validation

To verify the CFD code, the results were compared with published experimental data [17]. The numerical simulation was conducted using the geometry presented in the literature. Fig. 3 shows the solid mass flux profile in a pneumatic transport reactor at a height 3.9 m; the red triangles correspond to experimental results and the black line represents numerical simulation data using the method described above. The numerical simulation data are comparable to the experimental results.

3.3 Operating conditions for a pneumatic transport reactor

The CO_2 capture process involves two reactors, as shown in Fig. 1. The bench-scale carbonation reactor [6, 8] used in this study was 6.8 m high and 0.07 m in diameter; the reaction heat.

exchanger is at the bottom of the reactor and the sensible heat exchanger is at the top [6]. The superficial velocity of the pneumatic transport reactor must exceed the minimum transport velocity (U_{mt}) of the solid. Using Eq. (2) above, U_{mt} = 1.94 m/s [11]. Considering this, the superficial velocity was set at 2.5 m/s. In Fig. 2, the red circles show the flow regime under the conditions used in this study; the conditions overlapped with fluidization and pneumatic transport. Geometric information and the physical and thermal properties of the gas and solid are listed in Table 2. In the comparative study with a single-phase gas, a simulation of a reactor without particles was conducted using the same velocity conditions.

Table 2. Physical and thermal properties and boundary conditions of a pneumatic transport reactor.

Parameter	Value	Parameter	Value
Gas density (kg/m³)	1.131	Superficial velocity (m/s)	2.5 m/s
Gas viscosity (Pa·s)	1.904×10^{-5}	Gas temperature at inlet (K)	313
Gas thermal conductivity (W/m K)	0.0272	Solid flux (kg/m²s)	3.6/0
Gas specific heat (J/kg K)	1005.6	Solid temperature at inlet (K)	313
Solid density (kg/m³)	1770	Cooler temperature (K)	293
Particle dimeter (μm)	100	Riser diameter (m)	0.07
Solid thermal conductivity (W/m K)	4	Riser height (m)	6.8
Solid specific heat (J/kg K)	1140	Heat exchange height (m)	4

4. Results and discussion

4.1 Pressure difference

In a pneumatic transport reactor, the pressure difference of the reactors is an important indicator of the characteristics of the gaseous environments [18]. Fig. 4(a) shows that the pressure difference of the pneumatic transport reactor exceeds that of single-phase gas flow. For an analysis of this result, the basic pressure loss equation is expressed as follows [19]:

$$\frac{\Delta P}{L} = \rho_g \varepsilon g + \rho_p (1-\varepsilon) g + \frac{f_s \rho_p (1-\varepsilon) u_p^2}{2D} + \frac{2 f_g \rho \varepsilon u_g^2}{2D}. \quad (5)$$

The term on the left side of the equation is the pressure loss. The terms on the right side of the equation are the gas gravity, solid gravity, solid friction effect, and gas friction effect, respectively. Generally, both friction effects are negligible compared with the gravity terms. The solid density is more than 1000 times the gas density. However, pneumatic transport flow is dilute flow and its voidage exceeds 0.95. The increment in the overall pressure of pneumatic transport is mainly due to the difference in gravity of the solid particles, because the gas gravity is nearly the same as single-phase gas flow. In addition, due to the random motion of particles, the pressure appears unstable; thus, the standard deviation of pressure is used, as shown in Fig. 4(b). This confirmed that there was no difference in the standard deviation of pressure up to a certain

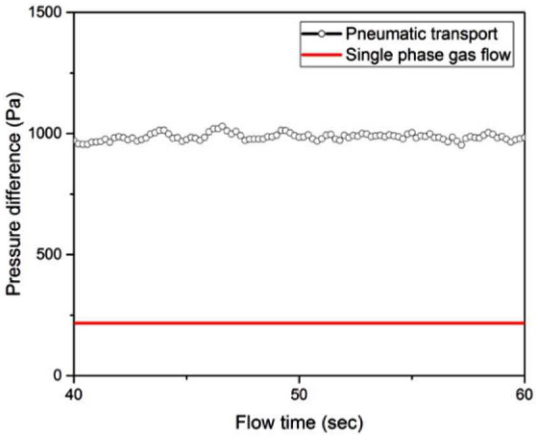

(a)

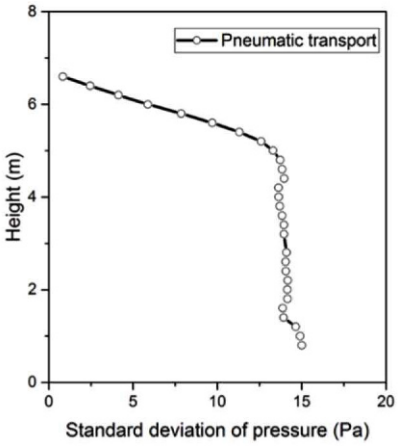

(b)

Fig. 4. Changes in (a) pressure; (b) the standard deviation of pressure with height (Time averaged: 20 s).

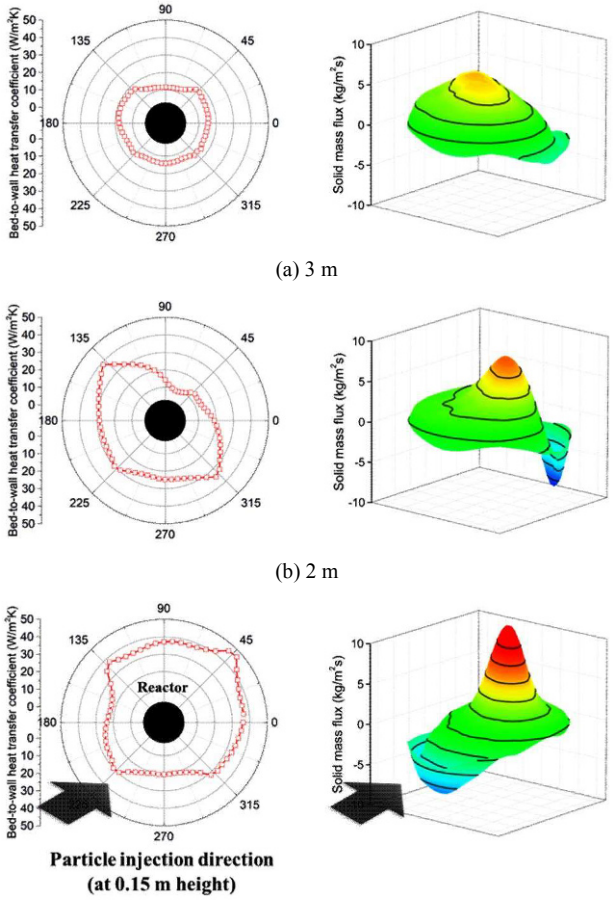

(a) 3 m

(b) 2 m

(c) 1 m

Fig. 5. Local bed-to-wall heat transfer coefficient and solid mass flux according to operating conditions at (a) 3 m; (b) 2 m; (c) 1 m (time averaged 20 s).

height from bottom, but it decreased in the vicinity of the exit. From the averaged pressure difference, the mean residence time of a particle can be expressed as follows [20]:

$$t_{m,p} = \frac{\text{Total solid mass in the reactor}}{\textit{Solid feed rate}} = \frac{\Delta P}{G_s g}. \quad (6)$$

By numerical analysis, the differential pressure is about 985 Pa and G_s is 3.6 kg/m^{2}s, as the operating condition. A simple calculation shows that the mean residence time $t_{m,p}$ is 27.91 s.

4.2 Particle behaviors

To gain insight into reactor phenomena, it is important to understand the behavior of the particles inside the reactor. In the experiments, it was difficult to quantify a vigorous gas-solid behavior that changes over time. Numerically, this behavior can be expressed in terms of the solid mass flux, as follows:

$$G_s = \rho_p (1-\varepsilon) g u_p. \quad (7)$$

Fig. 5 shows the solid mass flux at heights of 1, 2 and 3 m. When particles are introduced, the high gas velocity causes the particles to flow upward along the opposite wall where the solid injection port is located. As the height increases, that flow becomes weaker and relatively uniform.

4.3 Heat transfer coefficient

Heat transfer is important for continuous processes, including chemical reactions. To balance energy, the reactor thermal conditions must be maintained. In a pneumatic transport reactor, abrasion and corrosion are likely to occur because the particle velocity is high. As it is difficult to add an immersed heat transfer surface, the importance of bed-to-wall heat transfer increases.

Compared with single-phase gas flow, change in circumferential time average bed-to-wall heat transfer coefficient with height is high, as shown in Fig. 6. The surface average value of reaction heat exchanger was about 2 times larger than that of single-phase gas flow. Given that heat transfer is related to particle behavior in Fig. 5 [19], the bed-to-wall heat transfer

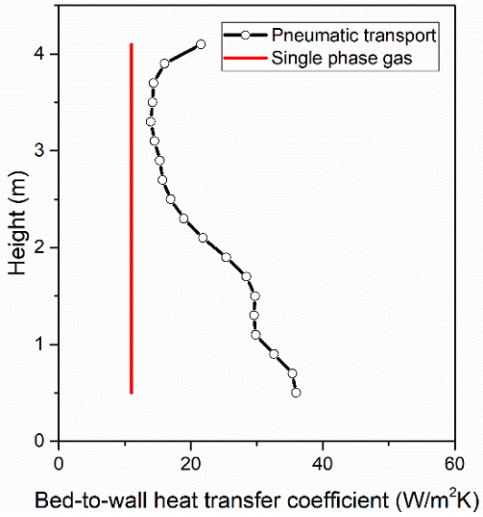

Fig. 6. Change in circumferential bed-to wall heat transfer coefficient with height (Time averaged: 20 s).

coefficient is uniform according to circumferential location at 3 m where the particles are well mixed. In contrast, the heat transfer coefficient is not uniform at 1 m and 2 m, in accordance with the non-uniformity of solid particle behavior. This means that when the radial mixing of the particles is poor, heat transfer coefficient is not uniform and has a bad effect for thermal design.

5. Conclusions

To enable continuous processing of a CO_2 capture reactor, it is necessary to analyze various considerations, such as pneumatic transport. This study analyzed a pneumatic transport reactor in terms of particle behavior and thermal dynamics.

First, our results confirmed that the pressure difference of the reactor was unstable due to the presence of particles. The degree of instability was expressed as the standard deviation of the pressure, which depended on the height within the reactor. The mean residence time of the particles was also calculated. The overall behavior of particles in the reactor was determined through an analysis of the pressure difference.

Second, the local behavior of particles in the reactor was quantified using the solid mass flux. When particles were introduced, the flow was not uniform to a certain height due to the location of injection.

Finally, from a thermal perspective, the area-averaged heat transfer coefficient is higher than that of single-phase gas flow in all areas. However, the heat transfer coefficient with circumferential location varies to a certain height due to the relationship between particle behavior and heat transfer. Above a certain height where the radial mixing of the particles is well, heat transfer coefficient with circumferential location is uniform.

The bed-to-wall heat transfer must be evaluated, to apply the pneumatic transport reactor for continuous CO_2 capture. As the heat transfer and gas-solid behavior results, pneumatic transport reactor can be evaluated whether this geometric design is sufficient for carbon capture system and whether the modification of reactor design is necessary.

Acknowledgment

This work was supported by the Korea CCS R&D Center (Korea CCS 2020 Project) grant funded by the Korea government Ministry of Science, ICT & Future Planning) in 2017 (KCRC-2014M1A8A1049330). This work also was supported by the Human Resources Development program (No. 20174030201720) of the Korea Institute of Energy Technology Evaluation and Planning (KETEP) grant funded by the Korea government Ministry of Trade, Industry and Energy.

Nomenclature

Ar	: Archimedes number
d_p	: Particle diameter [m]
d_p^*	: Non-dimensional particle diameter
e	: Coefficient of restitution
G_s	: Solid circulation rate [kg / m^{2}s]
g	: Gravity acceleration [m / s^2]
g_0	: Radial distribution coefficient
p	: Pressure [Pa]
Re_s	: Particle Reynolds number
T	: Temperature
U	: Velocity [m/s]
U^*	: Non-dimensional velocity
ε	: Volume fraction
θ	: Granular temperature
ρ	: Density [kg/m^3]
μ	: Viscosity [Pa s]

References

[1] IPCC, *Climate Change 2007: Synthesis Report*, Contribution of working groups I, II and III to the fourth assessment report of the intergovernmental panel on climate change, Geneva, Switzerland (2007).

[2] S. J. Davis, K. Caldeira and H. Damon Matthews, Future CO_2 emissions and climate change from existing energy infrastructure, *Science*, 329 (5997) (2010) 1330-1333.

[3] M. E. Boot-Handford et al., Carbon capture and storage update, *Energy Environ. Sci*., 7 (1) (2014) 130-189.

[4] N. MacDowell et al., An overview of CO_2 capture technologies, *Energy & Environmental Science*, 3 (11) (2010) 1645.

[5] S.-Y. Lee and S.-J. Park, A review on solid adsorbents for carbon dioxide capture, *Journal of Industrial and Engineering Chemistry*, 23 (2015) 1-11.

[6] Y.-K. Park et al., Energy recoverable multi-stage dry sorbent CO_2 capture process, *Energy Procedia*, 63 (2014) 2266-2279.

[7] I. Martínez et al., Review and research needs of Ca-looping systems modelling for post-combustion CO_2 capture applica-

tions, *International Journal of Greenhouse Gas Control*, 50 (2016) 271-304.
[8] H. Moon et al., Thermal design of heat-exchangeable reactors using a dry-sorbent CO_2 capture multi-step process, *Energy,* 84 (2015) 704-713.
[9] H. Yoo et al., Effect of a diffuser on gas-solid behavior in CFB riser for CO_2 capture, *Journal of Mechanical Science and Technology*, 30 (8) (2016) 3661-3666.
[10] H. Moon et al., Thermal-fluid characteristics on near wall of gas-solid fluidized bed reactor, *International Journal of Heat and Mass Transfer,* 114 (2017) 852-865.
[11] J. C. Yannopoulos, N. J. Themelis and W. H. Gavvin, An evaluation of the pneumatic transport reactor, *The Canadian Journal of Chemical Engineering*, 44 (4) (1966) 231-235.
[12] K. W. Chu and A. B. Yu, Numerical simulation of the gas-solid flow in three-dimensional pneumatic conveying bends, *Industrial & Engineering Chemistry Research*, 47 (18) (2008) 7058-7071.
[13] T. Li et al., Parameter sensitivity analysis on pressure drop of gas-solid flow for absorber sphere pneumatic conveying, *Energy Procedia*, 39 (2013) 12-19.
[14] H. T. Bi and J. R. Grace, Flow regime diagrams for gas-solid fluidization and upward transport, *International Journal of Multiphase Flow*, 21 (6) (1995) 1229-1236.
[15] L. G. Gibilaro et al., Generalized friction factor and drag coefficient correlations for fluid-particle interactions, *Chemical Engineering Science*, 40 (10) (1985) 1817-1823.
[16] D. J. Gunn, Transfer of heat or mass to particles in fixed and fluidised beds, *International Journal of Heat and Mass Transfer*, 21 (4) (1978) 467-476.
[17] T. Knowlton et al., Comparison of CFB hydrodynamic models. PSRI challenge problem, *InPSRI Challenge Problem Presented at the Eighth International Fluidization Conference,* Tour, France (1995).
[18] H. Yoo et al., Effect of the jet direction of gas nozzle on the residence time distribution of solids in circulating fluidized bed risers, *Journal of the Taiwan Institute of Chemical Engineers*, 71 (2017) 235-243.
[19] W.-C. Yang, *Handbook of fluidization and fluid-particle systems*, CRC press (2003).
[20] A. T. Harris, J. F. Davidson and R. B. Thorpe, Particle residence time distributions in circulating fluidised beds, *Chemical Engineering Science*, 58 (11) (2003) 2181-2202.

Seungyeong Choi received his B.S. degree (2016) from Yonsei University, Korea. He is a M.S. candidate in Mechanical Engineering at Yonsei University. His current research interests are on the heat transfer in fluidized bed reactor for CO_2 capture.

Hoanju Yoo received his B.S. degree (2009) and M.S. degree (2016) from Yonsei University, Korea. He is currently an Engineer at Korea Aerospace Industries (KAI) LTD. in Sacheon, Korea.

Hokyu Moon received his M.S. degree (2010) and Ph.D. (2016) from Yonsei University, Korea. Dr. Moon is currently a Senior Researcher at National Fusion Research Institute (NFRI) in Daejeon, Korea.

Hyung Hee Cho received his B.S. (1982) degree from Seoul National University, Korea. He received M.S. (1985) degree from Seoul National University and Ph.D. (1992) from Minnesota University, USA. Dr. Cho is currently a Professor at the School of Mechanical Engineering at Yonsei University in Seoul, Korea.